

Nonequilibrium radiation measurements and modelling relevant to Titan entry

A.M. Brandis¹, R.G. Morgan¹, C.O. Laux², T. Magin², T. McIntyre³ and P.A. Jacobs¹

¹Department of Hypersonics
 University of Queensland, Queensland, 4072 AUSTRALIA

²Laboratoire EM2C, CNRS UPR-288
 Ecole Centrale Paris, 92295 Châtenay-Malabry, France

³Department of Physics
 University of Queensland, Queensland, 4072 AUSTRALIA

Abstract

An update to a collisional-radiative model developed by Magin¹ for Huygens Titan atmospheric entry is proposed. The model is designed to predict the nonequilibrium populations and the radiation emitted from cyanogen and nitrogen during the entry of the Huygens probe into the Titan atmosphere. Radiation during Titan entry is important at lower speeds (around 5 – 6 km/s) more so than other planetary entries due to the formation of cyanogen in the shock layer, which is a highly radiative species. The model has been tested against measurements obtained with the EAST shock tube of NASA Ames Research Centre.^{1,2} The motivation for the update is due to the large discrepancies shown in the post-shock fall-off rates of the radiation when compared to the experimental EAST shock tube test results. Modifications were made to the reaction rates used to calculate the species concentrations in the flow field. The reaction that was deemed most influential for the radiation fall off rate was the dissociation of molecular nitrogen. The model with modified reaction rates showed significantly better agreement with the EAST data. This paper also includes experimental results for radiation and spectra for Titan entry. Experiments were performed on the University of Queensland's X2 expansion tube. Spectra were recorded at various positions behind the shock. This enabled the construction of radiation profiles for Titan entry, as well as wavelength plots to identify various radiating species, in this case, predominately CN violet. This paper includes radiation profiles to compare with experiments performed at NASA Ames. It is planned that further experiments will be performed to cover a larger pressure range than NASA Ames. Good qualitative agreement has so far been obtained between our data and NASA Ames, however, it should be noted at the time of printing, the experimental spectrum have not been calibrated absolutely.

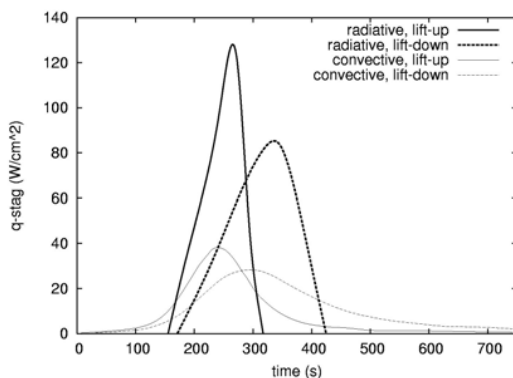


Figure 1 Heating rates during Titan aerocapture.³

Introduction

The design of aerocapture aeroshells for Titan atmospheric entry requires reliable estimates of the total heat transfer to the vehicle surface. Present estimates of the heat transfer from CFD analyses vary greatly,³ and design uncertainty factors related to thermal protection systems can be very large (over 100%) as discussed in Gnoffo et al.⁴ In the case of entry into the Titan atmosphere (predominantly nitrogen, small amounts of methane with traces of argon), the CN molecule forms in the nonequilibrium shock layer and this is known to be a strong radiator.³ However, the modelling associated with this strong CN radiator suffers from at least two difficulties: a) the kinetics of CN excited state populations are not well quantified,^{1,2,5} and b) given accurate CN excited states, there is disagreement in the literature about appropriate radiation transport models.^{5,6,7} The models used for the various processes and the coupling between various models have a strong influence on the predicted radiative heating levels. In order to reduce the uncertainty and variation among the CFD analyses, it is desirable to perform experiments that study the shock layer flow over aeroshell vehicles in a simulated Titan atmosphere. We propose that through the use of superorbital nonreflected shock tubes uncertainty reduction in radiation models can be achieved. Superorbital nonreflected shock tubes provide an impulsive test flow that can simulate the atmospheric entry flow conditions for a typical aerocapture manoeuvre. The experiments in the shock tube can provide measurements of total radiative intensity of the nonequilibrium reacting flow. These

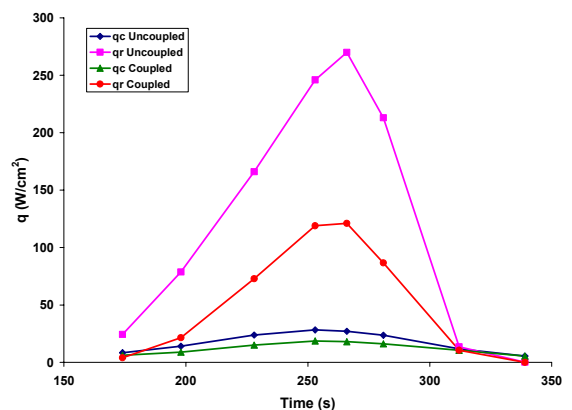


Figure 2 Stagnation-point convective and radiative heating as a function of time on the minimum atmosphere lift-up design trajectory.⁷

measurements will be valuable for validation of physical models for the CN radiation in the Titan shock layer flow.

During high speed entry into the Titan atmosphere, chemical kinetic analyses indicate that CN is formed in above equilibrium quantities in the nonequilibrium shock layer.³ Previous theoretical studies on the radiation experienced by a craft through a Titan atmosphere have shown the radiative heating rates to be around three to five times the peak convective heating rate.³ This can be seen in Figure 1. Results have shown the violet band of CN dominates the radiative heating rates. The heating has also been found to be very sensitive to dissociation of molecular nitrogen. As the dissociation of molecular nitrogen is a very important reaction in the radiation mechanism for Titan, improvements have been made to a collisional radiative model (CR). A vibrationally specific model for the dissociation of nitrogen has now been incorporated into the CR model. Through this improvement to the modelling of the reaction rates, it will provide better estimates of the concentrations of species in the flow and provide a good tool for comparison with the experimental results.

The primary focus of this paper is to report the development of the nitrogen vibrationally specific CR model and present the initial data from the qualitative X2 radiation intensity experiments. The following sections describe the testing facilities and the experimental spectroscopy set up. The preliminary data from the spectroscopy is presented along with comparisons to the EAST data.

Background

The space probe designer is ultimately interested in accurate numbers for total heat transfer to the aeroshell surface as this is what influences the heatshield design. The details of CN radiation modelling and its coupling to the flow dynamics are a means to an end in order to estimate the total heat transfer rates. To date there have been relatively few attempts to measure the radiative intensity of Titan entry conditions. We propose to measure the absolute radiative intensity. This will give CFD analyses some physical data against which to validate their models. The expansion tubes at UQ combine free piston driver techniques with expansion tube concepts to obtain superorbital velocities (>10 km/s). These extremely high speeds encountered during testing are used to model interplanetary entry conditions. The UQ expansion tubes are among the few facilities around the world capable of replicating these high velocity flows. The major

tube, acceleration tube, test section and dump tank. A schematic of one the expansion tubes, X2, is given in Figure 3 and the location of the pressure transducers shown in Table 1. The high velocities are usually established by means of an unsteady expansion process that takes place as the test gas is accelerated down a long tube. The acceleration tube has a bore of 85 mm. It should be noted that for the experiments conducted on X2 for radiation measurements, the set up of X2 was modified. There was no secondary diaphragm used, so therefore the acceleration tube was used as an extension to the shock tube, as shown in Figure 4. This effectively turns X2 into a nonreflected shock tunnel (NRST). Alternatively, the shock tube may be used as a shock heated driver for very high shock speeds.

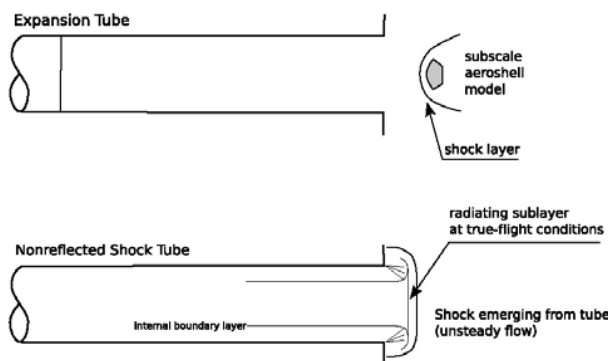


Figure 4 Expansion tube vs Nonreflected shock tube set up

Vibrationally Specific CR Model

An electronic collisional-radiative model was developed by Thierry Magin¹ to predict the nonequilibrium populations and the radiation of the excited electronic states CN(A,B) and N₂(A,B,C)¹. The kinetic mechanism comprises spontaneous emission of the excited states, excitation-deexcitation by nitrogen and electron-impact collisions, pooling of N₂(A), and quenching of N₂(A) by excitation of CN(X) to CN(B)¹. The model was compared to the experimental data from NASA Ames EAST facility. From the simulations run, it appeared that there was a significant discrepancy relating to the fall off rate of the simulations, see Figure 6. It was suggested that the reasons for the discrepancies were related to the reaction rates used in the simulation. From parametric variation of the reaction rates from the Gokcen 19 species Titan model,¹⁰ it was found that the molecular dissociation of nitrogen was the most influential reaction rate. This is to be expected, as the formation of N atoms is the precursor to the CN molecule forming. It was decided to incorporate a vibrationally specific model to simulate the reaction of all the ground state vibrational levels of N₂, known

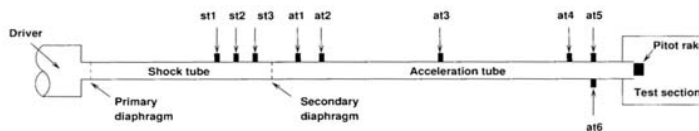


Figure 3 Schematic of classical X2 configuration⁹

Pressure Transducer Name	Distance from the Primary Diaphragm (m)	Pressure Transducer Name	Distance from the Primary Diaphragm (m)
st1	2.572	at3	6.019
st2	2.804	at4	7.865
st3	3.036	at5	8.045
at1	3.955	at6	8.045
at2	4.205		

Table 1 Location of flush mounted pressure transducers

components of all three of the currently operating machines (X1, X2 and X3) are the reservoir, driver, compression tube, shock

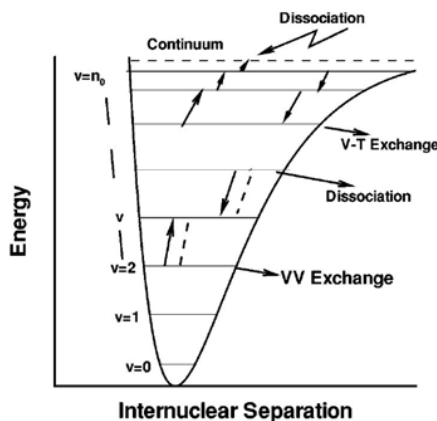


Figure 5 Dissociation energy profile¹¹

as the ViSpeN CR model (**V**ibrationally **S**pecific **N**itrogen). The N2 vibrationally specific model used was developed by Laurent Pierrot. This new model produces significantly better results in terms of the initial rise, absolute intensity level and fall off rates. This is due to each vibrational state of nitrogen having its individual reaction rate as opposed to an averaged rate for all states and that the higher level vibration states require less energy to dissociate, see Figure 5. Due to the flow being highly in nonequilibrium it is expected that distribution of N2 vibrational states also be in nonequilibrium.

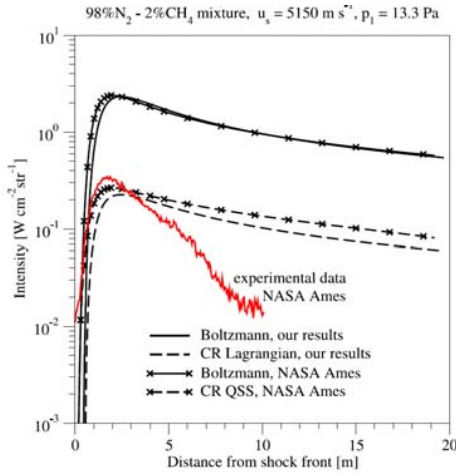


Figure 6 EAST experimental data vs simulations^{1,2}

The shock code of Magin¹ was modified to include the reaction rates calculated by Pierrot¹² for the dissociation of molecular nitrogen. For each time step, a section of Pierrot's code is run that calculates the vibrationally specific reaction rate based on the current temperature. So this means that the reaction $N_2 + M = N + N + M$ (where $M = N_2, N, N+, N_2+, e-$) does not use the reaction rate specified in Gokcen's 19 Titan species model. This reaction was deemed the most influential due to initial work where Gokcen's reaction rates were modified to observe their influence on the radiation profile. It was deemed that this reaction was most influential, and thus further work was focused on this reaction.

Pierrot's program takes into account all significant collisional and radiative processes in nitrogen, and considers separately the vibronic levels of molecules.^{1,12} The CR code by Magin is in two parts. The first calculates the flow field in a shock tube, not including radiation phenomena. The second uses this flow field information to calculate the nonequilibrium populations of the excited electronic levels for a nitrogen-methane mixture. The populations of excited electronic levels are obtained through the use of a Lagrangian flow solver¹.

The basic premise behind the vibrationally specific nitrogen CR is to analytically calculate the rate for the reaction of the nitrogen molecule in the ground state to the first vibrational state. Then all other reaction rates are scaled off this. The V-T reaction rates for the vibrationally specific nitrogen have been calculated with the following analytical expression⁸:

$$k_{1,0} = AT_g^n \exp\left(-\frac{B}{T_g^{1/3}} + \frac{C}{T_g^m}\right) \left[1 - D \exp\left(-\frac{E_{10}}{T_g}\right)\right]^{-1} \quad (1)$$

$$k_{v+1,v} = k_{1,0} G(v+1) \quad (2)$$

Using Schwartz-Slowsky-Herzfeld (SSH) theory and some approximations for the Morse oscillator model, $G(v+1)$ can be expressed as:

$$G(v+1) = \frac{(v+1)(1-x_e)}{1-x_e(v+1)} \frac{F(y_{v+1,v})}{F(y_{1,0})} \quad (3)$$

$$y_{v+1,v} = 0.32 E_{v=1,v} L \sqrt{\frac{\mu}{T_g}} \quad (4)$$

$$F(y) = \frac{1}{2} \left[3 - \exp\left(-\frac{2y}{3}\right) \right] \exp\left(-\frac{2y}{3}\right) \quad \text{for } 0 \leq y \leq 20$$

$$F(y) = 8 \left(\frac{\pi}{3}\right)^{1/3} y^{7/3} \exp(-3y^{2/3}) \quad \text{for } y > 20 \quad (5)$$

Another significant difference between Magin's results and the results of the updated program is the reaction rate for the dissociation of N2. The rate for dissociation in Thierry's model is based on an average temperature of $T_a = \sqrt{(T \times T_v)}$. The N2 dissociation rate in my model is taken from the vibrationally

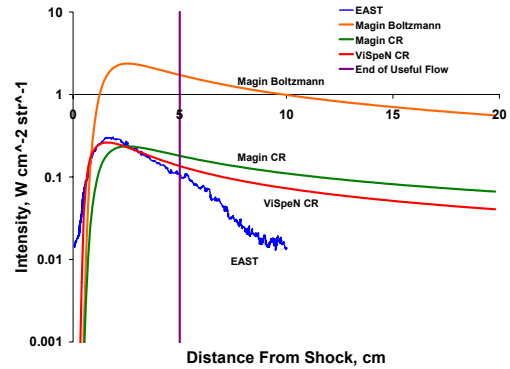


Figure 6 Comparison of previous data with new vibrationally specific model on a log plot

specific model of Laurent Pierrot. In this model both the gas temperature and vibrational temperature are taken into account, with assumptions made about the rotational, electron and electronic temperatures. According to Laurent Pierrot's report in section 2.4, 'Multi-temperature rate coefficients: influence of Tv', it is stated that "the temperature dependence postulated by Park provides reasonable agreement for a limited set of experiments in shock-heated air or nitrogen, we will see in the following that the temperature dependence of Park's rate coefficients is in general incorrect; this conclusion is independent of the value of q."¹² It is this different use of temperature

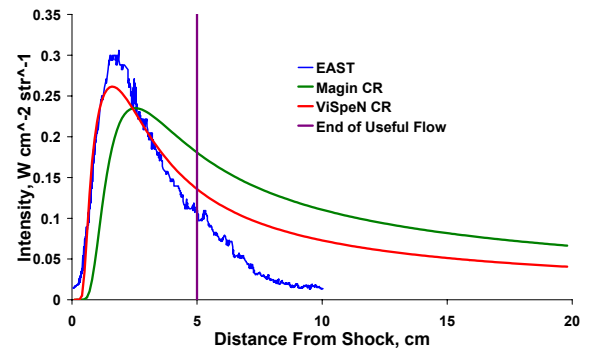


Figure 7 Comparison of previous data vs new vibrationally specific data on linear plot

assumptions that is the source of the discrepancy in the post-shock area where the difference between T and Tv is largest.

Simulation Results

This section presents some of the data from simulations run using the updated vibrationally specific collisional radiative program for Titan mixtures. Figure 6 shows the improvement of the updated model in comparison with Magin’s CR model and the NASA Ames EAST data. It can be seen that there is significant improvement to the model in terms of the initial rise, absolute intensity maximum and the fall off rates. This improvement is even more pronounced when viewed on a linear scale (see Figure 7). Especially when you consider that it is reported in the Ames paper that the experimental flow is of little use after 5 cm due to driver gas contamination. The reason for the faster initial rise, is to due the dissociation of nitrogen occurring faster in updated program. Therefore there are more nitrogen atoms in the flow to form cyanogen. This is reflected in the cyanogen peaking earlier in comparison to Magin’s model, see Figure 8.

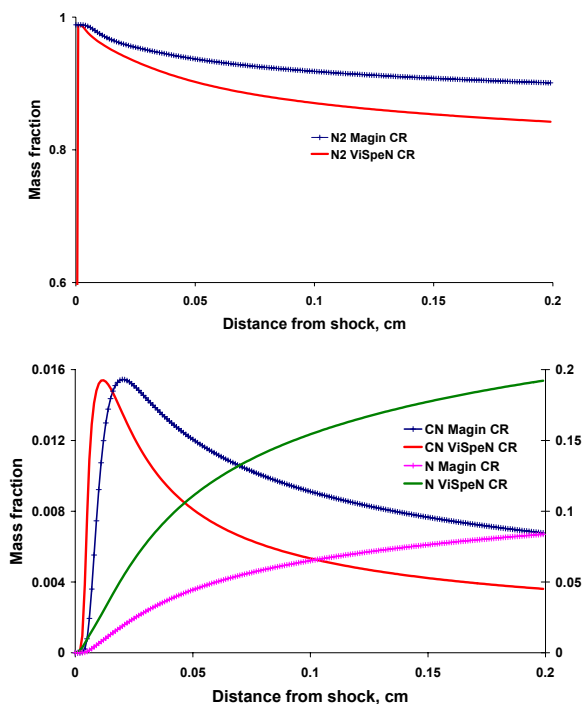
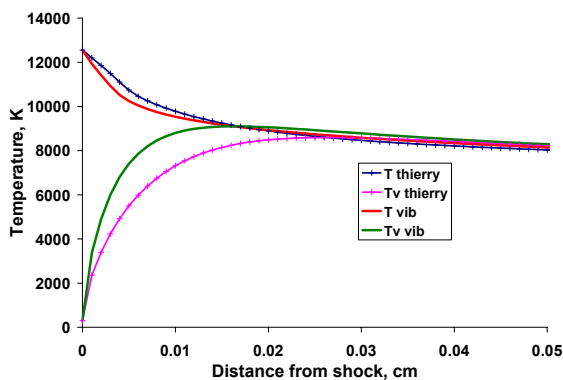


Figure 8 Species Concentration



The temperature profiles are also presented for the gas temperature and vibrational temperature. It can be seen that the vibrational temperature rises earlier and peaks at a higher value before reaching thermoequilibrium, see Figure 9.

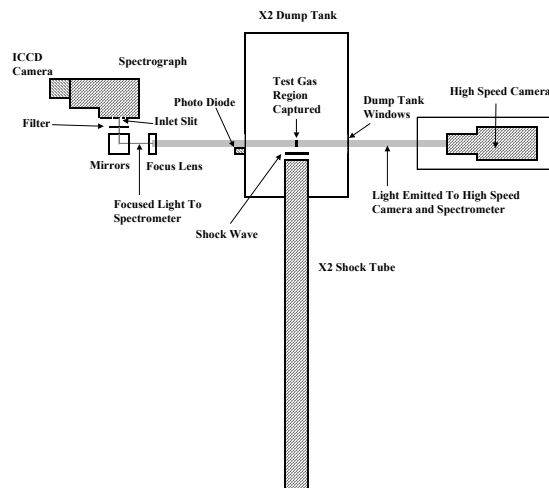
Facility/Test Conditions

The new experiments were carried out in the X2 expansion tunnel facility at the University of Queensland. Usually X2 is operated in expansion tunnel mode, however, for these experiments, the facility was modified to be operated in a non-reflected shock tunnel mode. This enabled the experiments to be performed with flow parameters close to Titan flight conditions.

For the experiments presented in this paper, the facility was configured as follows. The driver was 86% He and 14% Ar at a pressure of 300 mBar. The Titan gas used in these simulations was made up of 95% N2 and 5% CH4. The primary diaphragm separating these two was pre-scoured 1.2 mm steel. The shock tube fill pressure was 130 Pa. The spectrograph was set up approximately 750 mm from the test section. This resulted in a magnification of 3 times. The amount of flow captured in each spectrograph exposure was 23.8 mm in length. It is intended that for future experiments this length be increased. It is also intended that further tests will be performed with varying amounts of CH4 in the test gas, to approximate various altitudes at Titan.

Shock velocities of approximately 5.7 km/s were obtained for this testing. The test times for these shots were approximately 160 microseconds. This can be seen from the pitot traces obtained just downstream of the region captured in the spectroscopy. Furthermore, this can also be match with the luminosity data obtained for the high speed camera set up to capture each shot. The shock can be seen clearly on the camera footage, with a region of test gas following for a period of about 60 microseconds (corresponding to the steady region on the pitot traces), see Figure 14.

The spectrograph was initially being triggered off wall pressure gauge at6 (the last pressure transducer on the shock tube). However, this was changed to a more reliable technique of triggering off a photo diode attached to the outside of the dump tank. This photo diode triggering system enabled us to accurately capture the correct area of the flow we were interested in. The experimental set up can be seen in Figure 10. The 2D captured data gives intensity over a range of wavelengths at axial locations down the centre-line of the test section.



Experimental Results

Due to the images recorded by the ICCD cameras not being calibrated at the time of printing, the output intensity of these experiments is in the form of 'counts'. The shock velocities for the shots presented in this paper were $5.72 \pm 2\%$ km/s. The error in the ICCD measurements is about $30\%^2$. The raw data picture for each shot can then be summed either in distance (giving a spectrum intensity vs wavelength plot) or over all wavelengths (creating a radiation intensity profile). From the raw pictures and wavelength plots, CN violet can easily be seen. The three main vibrational states of CN are clearly identifiable in the spectrum. The predominant band is $\Delta v = 0$, and the smaller bands either side are $\Delta v = \pm 1$. At present, this is the only wavelength region to be examined.

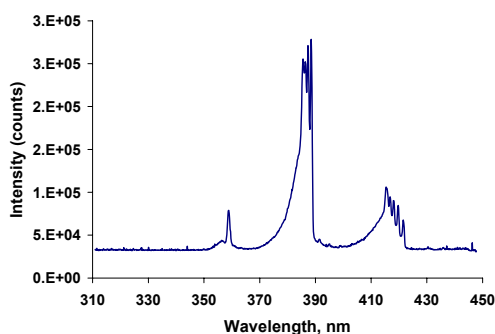


Figure 11 Wavelength profile for shot x2s405

Our initial data has been compared to the experimental data from NASA Ames. It can be seen that the general trend matches quite well. However, there are some discrepancies for the initial rise just behind the shock. These discrepancies will be further investigated. It also should be noted that we have quite good agreement between various shots. Due to NASA Ames recording a greater distance along the test-section centreline with their spectroscopy, our experiments were required to be performed several times so the entire intensity profile could be matched. Figure 11 shows a sample of a wavelength profile obtained from one experiment. The band structure of CN violet dominates the entire spectra. Figure 12 and 13 show a comparison between the EAST data and the intensity experiments performed on X2. It appears that the shock has not been captured as well during our experiments. A couple of proposed reasons for this are:

1. The shock has rounded by the time we record the spectra. This is possible as the spectra we have recorded is approximately 50 mm downstream of the shock tube exit,
2. There is some smearing of the shock wave due to exposure effects.

At the time of printing these are just our initial results. They do show promising signs. The agreement of the fall-off rate

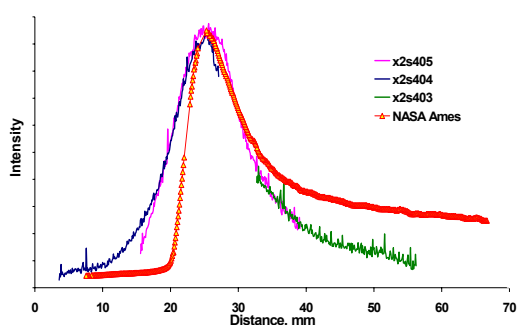


Figure 12 Comparison of X2 vs EAST radiation (130 Pa)

compared to the EAST data is very good. As is the general shape of the curve. As mentioned previously, the data has not yet been calibrated for absolute levels and so the data has been scaled so the peak intensity occurs at the same value.

Figure 14 shows a number of frames from the high speed camera. Various frames are shown, with their corresponding position shown on a Pitot trace. The Pitot trace has a great steady period of about 60 microseconds (so we have a slug length of radiating test gas of about 340 mm). The shock can be seen leaving the tube exit and traversing across the captured region. Behind the shock, the radiating test gas can be seen. As time progresses the intensity of the radiating test gas decreases, and this is reflected

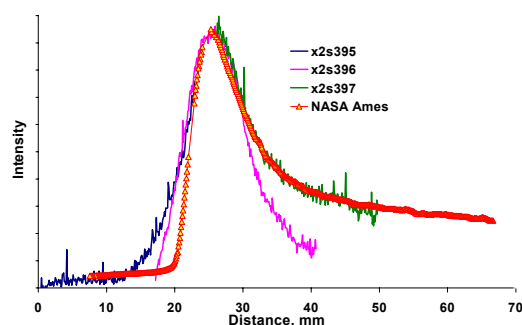
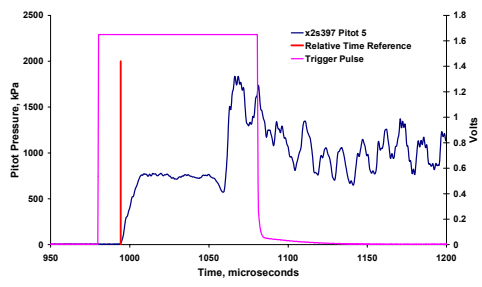


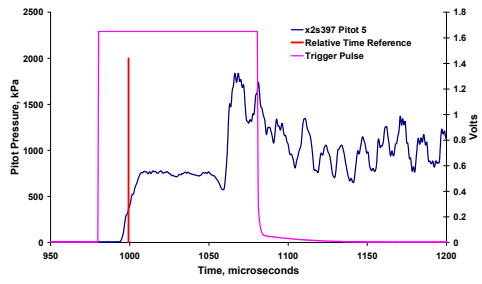
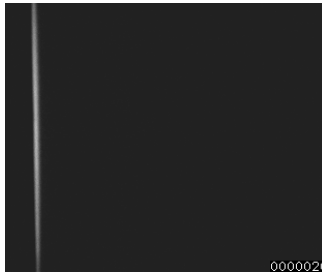
Figure 13 Comparison of X2 vs EAST radiation (260 Pa)

in the reducing light shown. In the last frame, the interface between the driver gas and test gas can be seen. This gives further validation to the test time of the experiment. The data from the high speed camera correlates very well with the pitot trace. It should be noted that the bright lines directly behind the shock are believed to be reflections off the far dump tank window. It should also be noted that the intensity settings had to be modified for some of the frames. This was due to the dramatic differences in light emitted during various times of the exposure. For the plots presented, 3 different brightness and contrast settings were used. The first three plots (a, b & c) had a low brightness due to the shock being in frame. The second two plots (d & e) had medium brightness with the strongly radiating test gas. The last frame (f) had maximum brightness so the interface between the driver and test gas could easily be seen.

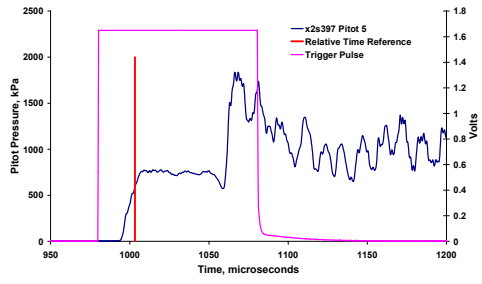
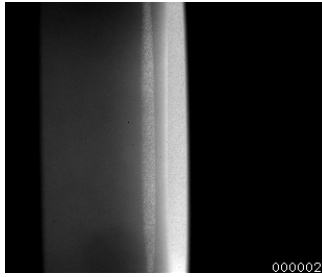
The raw picture taken by the spectrometer is shown in Figure 15 and 16. The bands of CN violet can be seen, as well as the CN violet $\Delta v = \pm 1$ bands. The top picture shows a shot where the peak was captured. The bottom picture shows a shot where the shock wave was captured, see Figure 15. CN violet profiles with respect to distance are shown in Figure 16. This is a very good plot to see the growth of the CN structure with respect to the distance from the shock.



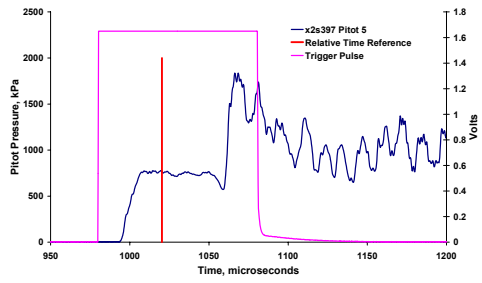
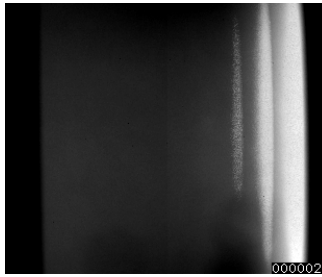
(a)



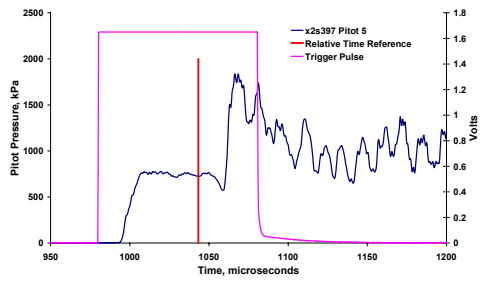
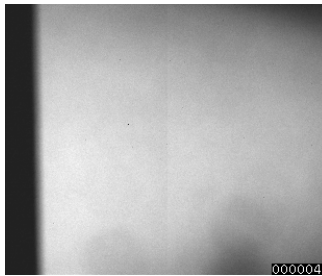
(b)



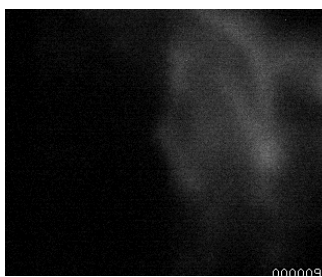
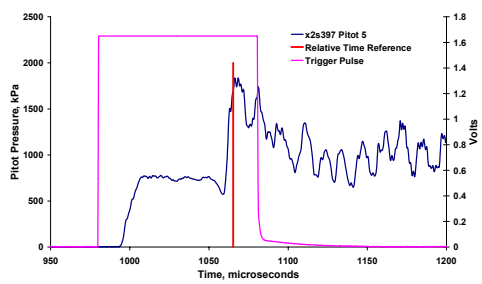
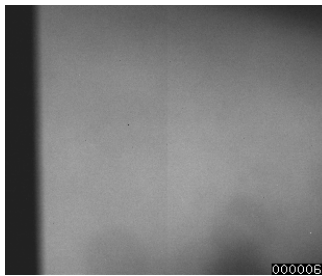
(c)



(d)



(e)



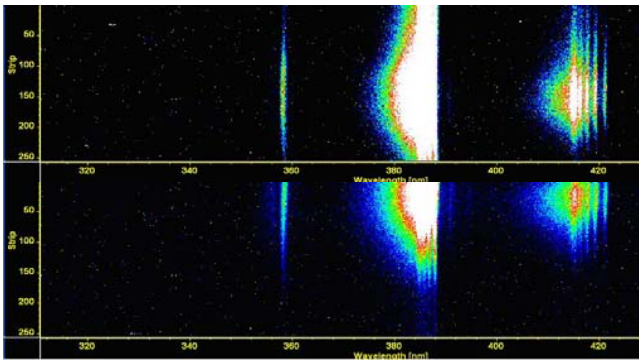


Figure 15 Distance vs Wavelength intensity pictures (shots x2s404, x2s405)

Future work

Currently the ViSpeN CR model only includes vibrational quantum jumps of one vibrational level (ie $\Delta v = \pm 1$). Through the work of Capitelli, Lino da Silva, Adamovich, Macheret^{13, 14, 15, 16} and others models have been developed to include Δv of greater than 1. It is proposed that this work will be incorporated into ViSpeN to make it more encompassing. The differences in reaction rate and temperature models will be further examined.

Calibration procedures will be developed and performed to obtain the absolute levels of the radiation intensity profile. This will enable direct comparisons with the EAST data. The optical set up will also be modified so a greater distance will be recorded by the spectrometer. Following the installation of the new optical set up, a new experimental campaign will be conducted to encompass various static pressures, shock speeds and Titan gas composition.

Conclusion

Large variations exist in predictions for radiation levels from CFD, and so experimental validation and a better understanding of the kinetics of CN excited populations is required. Our simulations with ViSpeN show greatly improved correlation with experimental data from NASA Ames EAST facility, and we have demonstrated a useful X-tube condition for analysing nonequilibrium radiation under Titan conditions. Furthermore, our preliminary experimental results for radiation intensity show promising results in terms of comparison with EAST data. The condition also shows excellent flow data. The pitot trace is very steady, resulting in about 340 mm of radiating test gas (further clearly verified by the high speed camera) and the CN wavelength profiles have a very good noise to signal ratio. Through the combination of spectroscopic work and radiation modelling at Ecole Centrale and UQ, combined with the shock tube work at UQ, significant insights into the Titan radiation problem will be achieved.

Acknowledgements

A UQ Graduate Research Student Travel Award (GRSTA) allowed Aaron Brandis to have an extended stay at Ecole Centrale Paris.

The experimental work in the X2 facility is supported by an Australian Research Council Grant and Queensland Smart State Research Facilities Fund.

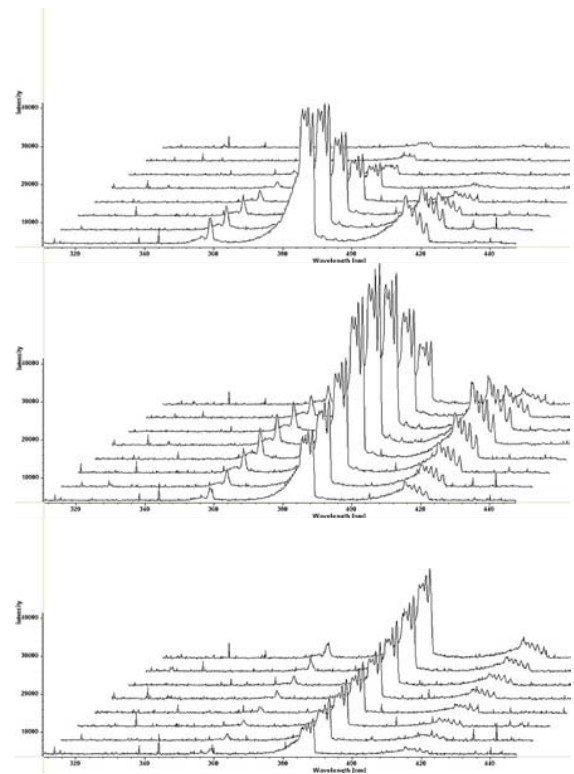


Figure 16 CN intensity profiles (shots x2s404, x2s405, x2s403)

References

- [1] Magin, T.E., Caillault, L., Bourdon, A. and Laux, C.O., *Nonequilibrium radiation modelling for Huygens entry*, Journal of Geophysical Research, Vol. 111, 2006..
- [2] Bose, D., Wright, M.J., Bogdanoff, D.W., Raiche, G.A. and Allen Jr, G.A., *Modeling and experimental validation of CN radiation behind a strong shock wave*, Paper AIAA-2005-768, 43rd AIAA Aerospace Sciences Meeting and Exhibition, 2005.
- [3] Olejniczak, J., Wright, M.J., Prabhu, D., Takashima, N., Zoby, V.E., Hollis, B.R. and Sutton, K., *An analysis of the radiative heating environment for aerocapture at Titan*, Paper AIAA-2003-4953, 39th Joint Propulsion Conference, 2003.
- [4] Gnoffo, P. A., Weilmuenster, K.J., Hamilton II, H.H., Olynick, D.R. and Venkatapathy, E., *Computational aerothermodynamic design issues for hypersonics vehicles*, Journal of Spacecraft and Rockets, Vol. 36, No. 1, 1999, pp. 21 – 43.
- [5] Johnston, C., Hollis, B.R., and Sutton, K., *Radiative heating methodology for the Huygens probe*, Joint Thermophysics and Heat Transfer Conference, 2006.
- [6] Osawa, H., Matsuyama, S., Ohnishi, N. and Sawada, K., *Comparative computation of radiative heating environment for Huygens probe entry flight*, Paper AIAA-2006-3772, Joint Thermophysics and Heat Transfer Conference, 2006.
- [7] Wright, M. J., Bose, D. and Olejniczak, J., *Impact of flowfield-radiation coupling on aeroheating for Titan aerocapture*, Journal of Thermophysics and Heat Transfer, Vol. 19 No 1, 2005, pp. 17-27.
- [8] Chauveau, S.M., Laux, C.O., Daniel Kelley, J. and Kruger, C.H., *Vibrationally-specific collisional-radiative model for nonequilibrium air plasmas*, 33rd AIAA Plasmadynamics and Laser Conference, 2002.
- [9] Scott, M. P., Morgan, R.G. and Jacobs, P.A., *A new single stage driver for the X2 expansion tube*, Paper AIAA-2005-

- 697, 43rd AIAA Aerospace Sciences Meeting and Exhibition, 2005
- [10] Gökçen, T., *N₂-CH₄-Ar Chemical kinetic model for simulations of atmospheric entry to Titan*, Paper AIAA 2004-2469. 37th AIAA Thermophysics Conference, 28 June-1 July 2004, Portland Oregon.
- [11] Josyula, E. and Bailey, W.F., *Reactive and nonreactive vibrational energy exchanges in nonequilibrium hypersonic flows*, Physics of Fluids, Vol 15, No 10, 2003, pp 3223 - 3235
- [12] Pierrot, L., *Chemical kinetics and vibrationally-specific collisional-radiative models for nonequilibrium nitrogen plasmas*, Final Report of ESA Post-doctoral Fellowship, July 1999.
- [13] Capitelli, M., Colonna, G. and Esposito, F., *On the coupling of vibrational relaxation with the dissociation-recombination kinetics: from dynamics to aerospace applications*, Journal of Physical Chemistry, Vol 108, 2004, pp 8930 – 8934
- [14] Lino da Silva, M., Guerra, V. and Loureiro, J., *Nonequilibrium dissociation processes in hyperbolic atmospheric entries*, Journal of Thermophysics and Heat Transfer, 2006
- [15] Lino da Silva, M., Guerra, V. and Loureiro, J., *State-resolved dissociation rates for extremely nonequilibrium atmospheric entries*, Journal of Thermophysics and Heat Transfer, 2006
- [16] Macharet, S.O. and Adamovich, I.V., *Semiclassical modelling of state-specific dissociation rates in diatomic gases*, Journal of Chemical Physics, Vol 113, No 17, 2000, pp 7351 - 7361